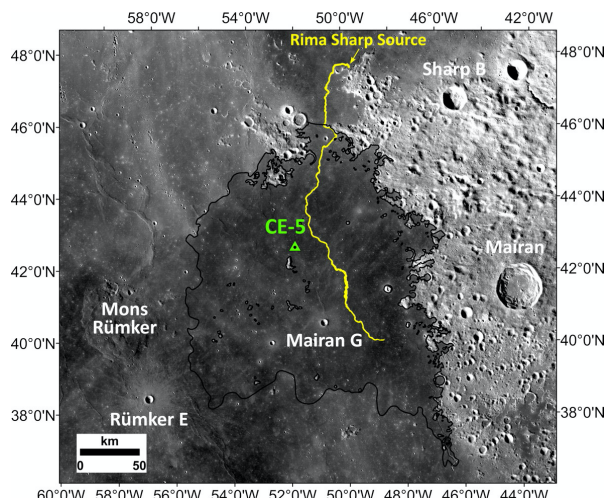


**MODELING THE ERUPTION OF THE LAVAS SAMPLED BY THE CHANG'E 5 MISSION.** Lionel Wilson<sup>1,2</sup>, James W. Head<sup>2</sup>, Yuqi Qian<sup>2,3</sup> and Long Xiao<sup>3</sup>, <sup>1</sup>Lancaster Environment Centre, Lancaster Univ., U.K. <sup>2</sup>Dept. of Earth, Environmental, and Planetary Sciences, Brown Univ., U.S.A. <sup>3</sup>Planetary Science Institute, China University of Geosciences, Wuhan, China.

**Introduction:** We model the emplacement of the young [1, 2] large-volume lunar lava flow Em4/P58 [3, 4] (Figure 1) sampled by the Chang'e-5 mission [5], and the Rima Sharp sinuous rille incised into the flow [6, 7].



**Figure 1.** Extent of the main part of the Em4/P58 flow and path of the Rima Sharp rille incised into it.

We interpret the morphology [6, 7] to imply that the rille formed by thermo-mechanical erosion of the upper surface of the lava flow during the closing stage of a single eruption. The large lava volume implies a high magma eruption rate [8, 9]. The high temperature and discharge rate of low-viscosity lava leaving the vent made its motion turbulent [10]. Consequent fast cooling while turbulence persisted generated bulk rheological properties very different from those of laminar lava flows. Rapid cooling during emplacement followed by much slower cooling to ambient should be reflected in returned sample petrology.

**Eruption scenario implied by morphology:** The ~270 km long Em4/P58 lava erupted from a vent system at the south end of Sinus Roris [6, 7]. Its mean thickness, area and volume are ~50 m, ~33,200 km<sup>2</sup> and ~1660 km<sup>3</sup> [6, 7]. It flowed to the north and ponded around the vent before flowing south and spreading laterally to pond again as a 20 m deep flow in a depression in the Northern Oceanus Procellarum between Mons Rümker and the Mairan crater (Fig. 1) [6, 7]. We infer that the flow then inflated to its present 50 m thickness as magma was intruded laterally into it near its base.

As the volume flux decreased, the fissure vent length decreased, and magma intrusion inflating the flow became more difficult. The magma level rose in the conduit until lava flowed out onto the surface of the

inflated flow. This late-stage overflow thermo-mechanically eroded the Rima Sharp rille channel. Figure 2 shows elevation data for Rima Sharp, measured along its meandering thalweg [6], which was used to find the slope  $\alpha$  of the surface being traversed by the rille-forming flow: 0.002 radians shallowing to 0.0004 radians in the depression. Figure 2 also shows the variation of the depth and width of the rille. The channel is 300 m deep at its source and 700 m wide, which we take to be an estimate of the width of the late-stage flow forming the rille.

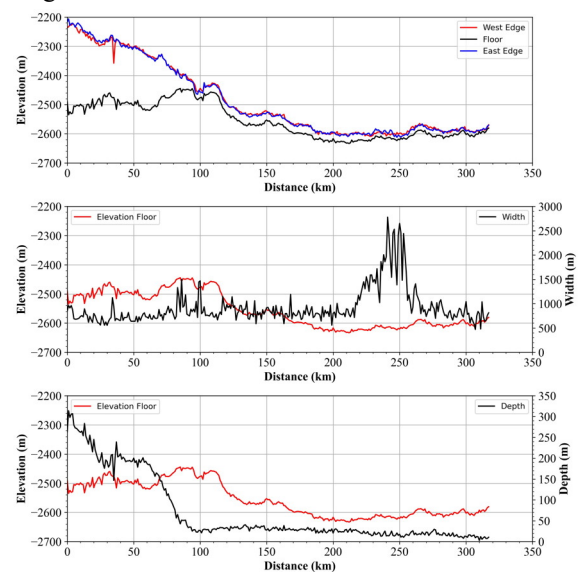


**Figure 2.** Elevation, depth and width measurements for Rima Sharp [6].

The ~1660 km<sup>3</sup> volume of the Em4/P58 flow implies [7] that the eruption resulted from the propagation directly to the surface of a large dike that formed in the partial melt zone at the top of a deep mantle diapir [8]. Initial magma discharge rates from such dikes can be at least  $3 \times 10^6 \text{ m}^3 \text{ s}^{-1}$  [8] and are likely to decline to  $\sim 3 \times 10^4 \text{ m}^3 \text{ s}^{-1}$  over a period of several days [9]. With rise speeds through the lithosphere of 10-20 m s<sup>-1</sup> [8], magma suffers little heat loss and erupts at near-liquidus temperature with a low viscosity. Models of eruptions of basaltic magma with these properties [8, 10-12] all show that at volume eruption rates of  $10^6$ - $10^5 \text{ m}^3 \text{ s}^{-1}$  the resulting lava flows must be turbulent.

**Dynamic eruption model:** Turbulence effectively homogenizes the lava temperature in a flow. Heat lost by conduction at the base is small [10] and radiation from the surface dominates heat loss. The temperature,  $T$ , varies with distance,  $x$ , along the flow as

$$dT/dx = -(s \varepsilon T^4) / (\rho c U D) \quad (1)$$

[10], where  $s$  is the Stefan-Boltzmann constant,  $5.67 \times 10^{-8} \text{ W m}^{-2} \text{ K}^{-4}$ , and  $\varepsilon$ ,  $\rho$ ,  $c$ ,  $U$  and  $D$  are the emissivity, bulk density, specific heat, mean speed, and thickness of the lava, respectively. We adopt  $\varepsilon = 0.96$  [13].  $\rho$  and  $c$  are functions of the temperature-controlled crystal content,  $X$ , of the lava, derived from compositional data [14] using MELTS software [15]. Crystal formation increases the viscosity of the lava and leads to non-Newtonian rheology. We model the lava as a Bingham plastic [16] with yield strength  $Y$  and plastic viscosity  $\eta$ . Using experimental data [17-19]:

$$Y = 0, X < 0.021 \quad (2)$$

$$Y = 2.95 \times 10^{-4} \{[(X/0.021) - 1] / [1 - (X/0.45)]\}^{3.509}, X > 0.021 \quad (3)$$

$$\eta = f_v (1477.15 / T)^{10.0207} \quad (4)$$

$$f_v = [1 - (X / 0.6)]^{-2.5}, X < 0.317 \quad (5)$$

$$f_v = \exp\{[2.5 + (X/(0.6 - X))^{0.48}] (X/0.6)\}, X > 0.317 \quad (6)$$

While the flow is fully turbulent,  $U$  is given by

$$U = [(2 g D \sin \alpha) / f_f]^{1/2} \quad (7)$$

The Fanning friction factor  $f_f$  can be expressed in terms of the flow Reynolds number  $Re$  by [15]

$$f_f = 0.001337 + 0.1226 Re^{-0.32} \quad (8)$$

After the flow becomes laminar a rigid plug forms in the upper part of the flow where the shear stress is less than the yield strength, and  $U$  is given by

$$U = [(\rho g D^2 \sin \alpha) / (6 \eta)] (2 - 3j + j^3) \quad (9)$$

where  $j = Y/(\rho g D \sin \alpha)$  is the fractional flow depth occupied by the plug.  $Y$  and  $\eta$  influence the flow regime via the Reynolds number,  $Re = (4 \rho U D)/\eta$ , and the Hedström number,  $He = (16 D^2 Y \rho) / \eta^2$ . Decreasing  $T$  increases  $X$ , which increases  $He$ , which increases the critical Reynolds number,  $Re_{crit}$ , allowing turbulence. Simultaneously, increasing  $X$  causes a decrease in  $Re$  from its initially high value. When  $Re$  is  $< Re_{crit}$ , turbulence ceases, the flow becomes laminar, and thermal boundary layers grow at all flow margins. The isothermal core of the flow is insulated and preserves the extremely non-Newtonian rheology that it had at the moment of turbulent-to-laminar transition.

**Results:** We fit the above model first to the main Em4/P58 flow. Using [8], the  $\sim 1660 \text{ km}^3$  lava volume [7] implies an initial magma flux of between  $5$  and  $6 \times 10^6 \text{ m}^3 \text{ s}^{-1}$ , decaying to  $\sim 5 \times 10^4 \text{ m}^3 \text{ s}^{-1}$  after 136 hours (5.7 days). The initially turbulent flow first became laminar 142 km from the vent after 8 hours having cooled by 81 K from its 1438 K eruption temperature and reached its maximum 270 km extent after 38 hours with the turbulent- laminar transition at that time being 130 km from the vent. The flow inflated by  $\sim 30 \text{ m}$  over the next 98 hours to reach its final  $\sim 50 \text{ m}$  thickness and radiative cooling formed a solid crust 0.47 m thick. The crust's surface temperature was  $\sim 393 \text{ K}$  and its base

temperature was equal to that of the turbulently cooled lava, 1357 K.

Finally, an overflow from the now very short ( $\sim 2 \text{ km}$  long) fissure vent produced a new flow on the surface of the inflated flow. This new flow was  $\sim 700 \text{ m}$  wide and erupted at  $\sim 5 \times 10^4 \text{ m}^3 \text{ s}^{-1}$  for at least 57 days. It was turbulent for a distance of  $\sim 80 \text{ km}$  from the vent along its meandering thalweg and thermo-mechanically eroded the Rima Sharpe channel to the depths shown in Fig. 2 at a maximum vertical erosion rate of  $75 \mu\text{m s}^{-1}$ . This erosion rate is 1.5 orders of magnitude greater than values found for erosion of cold bedrock [12, 13] because what was being eroded was the still partially-molten core of the Em4/P58 flow. The new flow eroded  $\sim 17 \text{ km}^3$  of the Em4/P58 flow, becoming  $\sim 7\%$  contaminated in the process, and the resulting  $\sim 247 \text{ km}^3$  of lava was emplaced beyond the distal end of the initial Em4/P58 flow.

**Implications for Chang'e 5 samples:** The location of the Chang'e-5 lander implies that it sampled the upper few meters of the Em4/P58 flow [20], lava that cooled at  $10 \pm 5 \text{ K/hour}$  from close to its 1438 K liquidus to 1357 K as it was emplaced, reaching  $\sim 35\%$  crystallinity in the process. The lava then cooled to lunar ambient over the next  $\sim 120$  years, completing its crystallization at a cooling rate of  $9 \pm 3 \text{ K/year}$ . The slow cooling rate and thick lava flow suggest that extensive fractional crystallization [21] is possible for the Chang'e-5 basalts.

**Implications for sinuous rilles in general:** The Chang'e 5 mission data have also provided significant insight into lunar sinuous rille formation. Eighty % of lunar sinuous rilles have depths  $< 110 \text{ m}$  and 90% are  $< 150 \text{ m}$  deep [20]. At erosion rates of  $1 \mu\text{m s}^{-1}$  [12, 13] these rille depths require eruptions lasting 3.7 and 5 years. We strongly suspect that the deepest lunar rilles are eroded into ponded lava forming the opening phase of a single eruption, as proposed here for Rima Sharp.

**References:** [1] Che X. et al. (2021) *Science*, 374, 887-890. [2] Li Q. et al. (2021) *Nature*, 600, 54-58. [3] Qian Y. et al. (2018) *JGR-Planets*, 123(6), 1407. [4] Hiesinger H. et al. (2011) *Spec. Pap. GSA*, 477, 1. [5] Zhou C. et al. (2021) *Adv. Sp. Res.* 69, 823-836. [6] Qian et al. (2021) *GRL*, 48, e2021GL092663. [7] Qian Y. et al. (2021) *EPSL*, 555, 116702. [8] Wilson L. & Head J. W. (2017) *Icarus*, 283, 146. [9] Wilson L. & Head J. W. (2018) *GRL*, 45, 5852. [10] Hulme G. (1973) *Mod. Geol.*, 4, 107-117. [11] Wilson L. & Head J.W. (1981) *JGR*, 86, 2971. [12] Williams D. A. et al. (2000) *JGR*, 105, 20,189. [13] Davies A. G. et al. (2011) *GRL*, 38, L21308. [14] Li C. et al. (2021) *Natl. Sci. Rev.*, nwab188 [15] M. Norman pers. comm. 2021. [16] Skelland A. H. P. (1967) *Non-Newtonian Flow and Heat Transfer*. Wiley. [17] Jeffrey D. J. & Acrivos A. (1976) *AICE Journal* 22(3), 417. [18] Pinkerton H. & Stevenson R. J. (1992) *JVGR* 53, 47. [19] Ishibashi H. & Sato H. (2010) *J. Min. Pet. Sci.* 105, 334. [20] Qian et al. (2021) *GRL*, 48, e2021GL095341. [21] Tian et al. (2021) *Nature*, 600, 59-63.